**PAPER** • **OPEN ACCESS**

# Example of bispectral analysis of a transmission line pylon

To cite this article: M. Esposito Marzino *et al* 2024 *J. Phys.: Conf. Ser.* **2647** 242013

Journal of Physics: Conference Series **2647** (2024) 242013 doi:10.1088/1742-6596/2647/24/242013

# Example of bispectral analysis of a transmission line pylon

**M. Esposito Marzino[1], T. Bastin[2], Y. Duchene[2], V. Denoël[1]**

[1]Structural & Stochastic Dynamics, Structural Engineering Division, University of Liège, Liège, Belgium
[2]Bureau Greisch, Allée des Noisetiers 25, 4031, Liège, Belgium

E-mail: michele.espositomarzino@uliege.be; tbastin@greisch.com; yduchene@greisch.com; v.denoel@uliege.be

**Abstract.** It is common practice to tackle buffeting analysis by means of spectral analysis, assuming a Gaussian context. However, natural actions, as wind, or wave loading, might sometimes show important non-Gaussian behaviour. This is known to have an important impact on the extreme values of such random processes. In this context, a non-Gaussian bispectral turbulent wind analysis has been conducted on a transmission line pylon model. The non-Gaussian nature of the wind load is the result of the adoption of a nonlinear polynomial wind model applied to the Gaussian wind turbulent velocity components. Results of a stochastic dynamic analysis are compared with respect to their Gaussian counterpart, as well as to the Eurocode approach based on the equivalent static loads, which was also object of comparison of engineers in the original computation with respect to turbulent wind dynamic analysis. Importance of non-Gaussian nature of wind loading is highlighted, and considerations on why and when it should not be underestimated are discussed.

## 1. Introduction

Non-Gaussian nature of wind loading within the Atmospheric Boundary Layer (ABL) is increasingly been acknowledged. Some authors [1, 5] have discussed that wind pressure on structures might sometimes be far from being characterized by a Gaussian Probability Density Function (PDF), specially in the zones where the flow detaches from the surface, creating turbulent vortices, but also where the nonlinearity of the drag force on a body immersed in wind plays an important role. However, in practical applications, almost never these considerations have been taken into account, therefore always assuming turbulence as a Gaussian random process [2, 6]. Indeed, in case of linear mechanical structural behavior, the structural response will also be Gaussian [5]. In this paper, bispectral analysis is developed and employed to a transmission line pylon model. These results will be compared and discussed with respect to the approaches commonly used up to now when dealing with wind loading. In this specific case, both the Eurocode approach based on the computation of some equivalent static wind loads, as well as the spectral analysis are included, since both were object of study when this model was originally developed. Final illustrations will show the motivations and remark the importance of bispectral analysis for turbulent winds.

## 2. Non-Gaussian winds: bispectral analysis

In buffeting analysis, the dynamic motion of the system is governed by the general equations

$$\mathbf{M}\ddot{\mathbf{x}}(t) + \mathbf{C}\dot{\mathbf{x}}(t) + \mathbf{K}\mathbf{x}(t) = \mathbf{f}(t) \tag{1}$$

For convenience, in structural analysis, good practice suggests, when possible, to project (1) in the modal basis $\mathbf{\Phi}$. This is particularly useful in case of proportional structural damping $\mathbf{C}$, in which case the projection operation onto such base results into a number NM of uncoupled equations:

$$\mathbf{M}^\star\ddot{\mathbf{q}}(t) + \mathbf{C}^\star\dot{\mathbf{q}}(t) + \mathbf{K}^\star\mathbf{q}(t) = \mathbf{p}(t) \tag{2}$$

where $\mathbf{M}^\star = \mathbf{\Phi}^T\mathbf{M}\mathbf{\Phi}$, $\mathbf{C}^\star = \mathbf{\Phi}^T\mathbf{C}\mathbf{\Phi}$, $\mathbf{K}^\star = \mathbf{\Phi}^T\mathbf{K}\mathbf{\Phi}$ are the diagonal modal mass, damping and stiffness matrices, $\mathbf{q}(t)$ the modal responses, and $\mathbf{p}(t) = \mathbf{\Phi}^T\mathbf{f}(t)$ the vector of modal loads, NM the number of kept vibration modes. Usually, (2) is solved by means of a spectral analysis [8], which relates the Power Spectral Density (PSD) of the response to the PSD of the wind load as:

$$\mathbf{S}_Q(\omega) = \mathbf{H}(\omega)\mathbf{S}_P(\omega)\mathbf{H}^*(\omega) \tag{3}$$

where

$$\mathbf{H}(\omega) = \left(-\mathbf{M}^\star\omega^2 + i\omega\mathbf{C}^\star + \mathbf{K}^\star\right)^{-1} \tag{4}$$

is the Frequency Response Function, and the symbol $[\cdot]^*$ represents the complex and transposed operator. Integration along frequencies of (3) gives the second order statistical moment, namely variance (covariance) for auto- (cross-) elements of the 2D matrix of PSDs of modal responses $\mathbf{S_Q}(\omega)$:

$$\Sigma_{\mathbf{Q}} := \mathbf{m}_{2,Q} = \int_{-\infty}^{\infty} \mathbf{S}_Q(\omega)d\omega. \tag{5}$$

However, application of Eqs. (3) and (5) are exhaustive only in those contexts in which the input random process is known to have a Gaussian Probability Density Function (PDF). This is direct consequence of the fact that a Gaussian process can be fully characterized knowing its mean and variance. Whenever the input process is non-Gaussian, higher order statistics are needed in order to characterise it. In wind engineering, characterization up to third and fourth order moments are considered a good estimate. Therefore, at third order there exist similar equations [3, 2, 4] to express the bispectrum of modal responses $B_{Q_{mno}}(\omega_1, \omega_2)$ as a function of the bispectrum of modal loads:

$$B_{Q_{mno}}(\omega_1, \omega_2) = H_m(\omega_1)H_n(\omega_2)H_o^*(\omega_1 + \omega_2)B_{P_{mno}}(\omega_1, \omega_2). \tag{6}$$

where

$$H_i(\omega) = \frac{1}{m_i^\star\omega^2 + i\omega c_i^\star + k_i^\star} \tag{7}$$

is the $i$th mode frequency response function. The bispectrum integrated in the 2D space of frequencies gives the third statistical moment [4]

$$m_{3_{Q_{mno}}} = \int\int_{-\infty}^{\infty} B_{Q_{mno}}(\omega_1, \omega_2)d\omega_1 d\omega_2 \tag{8}$$

Combining Eqs. (5) and (8), the skewness coefficient reads

$$\gamma_{3,Q_{mno}} = \frac{m_{3_{Q_{mno}}}}{\sigma_{Q_m}\sigma_{Q_m}\sigma_{Q_o}}. \tag{9}$$

It quantifies the diversion of the PDF from a Gaussian-like having same mean and stardard deviation. Assuming the validity of the monotone region for the kurtosis coefficient, which has been proved to agree with Monte Carlo simulation in [3], model for estimating non-Gaussian peak factors and extreme values can be applied (e.g. [7]).

## 3. Inputs of the problem

### *3.1. Description of the structure*

One of the main motivations of this paper was indeed the application of bispectral wind turbulent analysis to a real structure, which would have already been designed to wind loading. Clearly, this choice is to ease comparison between common used approaches and the proposed one. The chosen structure refers to the highest among all the steel towers being part of a project of electric network extension via a new 400km line running through Netherlands and Germany, named Wintrack II. Greisch design office took part in the pre-design phase, from 2014 to 2016. The model used in this example therefore is the one they had developed for this phase. Figure 1 shows three images of the structure: the leftmost is a rendering showing the proposed real setup of the towers installation; the middle is a drawing with relative dimesions in a front view; the rightmost shows the beam model. The structure dimensions are: 71.2m of height; 2.5m base diameter, with 30mm thickness; 0.5m diameter at the top, with 8mm thickness. The main structural material is steel S235.

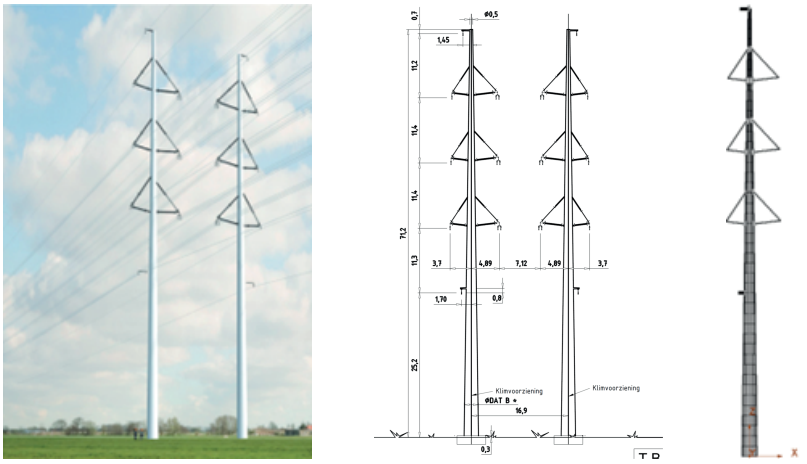


**Figure 1.** (a) Render of the two adjacent towers along the electric line; (b) sketch of the two towers in a front view; (c) view in the X-Z plan of the finite element model of the highest tower Tennet-W4S450 (71.2 m) generated by Greisch.

A modal analysis was conducted on the finite element model. Some values are reported in Table 3.1 for the first 4 modes of vibration, which for the shape of the considered structure, are (almost) symmetric along X and Y axes. A damping ratio of 0.3% for all vibration modes has been assumed. Mode shapes are normalized to a maximum unit displacement.

| Mode | Freq [Hz] | Modal mass [kg] | $\xi$ [%] |
|---|---|---|---|
| 1 | 0.8453 | 3302.7 | 0.3 |
| 2 | 0.8456 | 3315.4 | 0.3 |
| 3 | 2.3404 | 1547.1 | 0.3 |
| 4 | 2.3443 | 1572.9 | 0.3 |

**Table 1.** Modal structural data for its first 4 modes of vibrations.

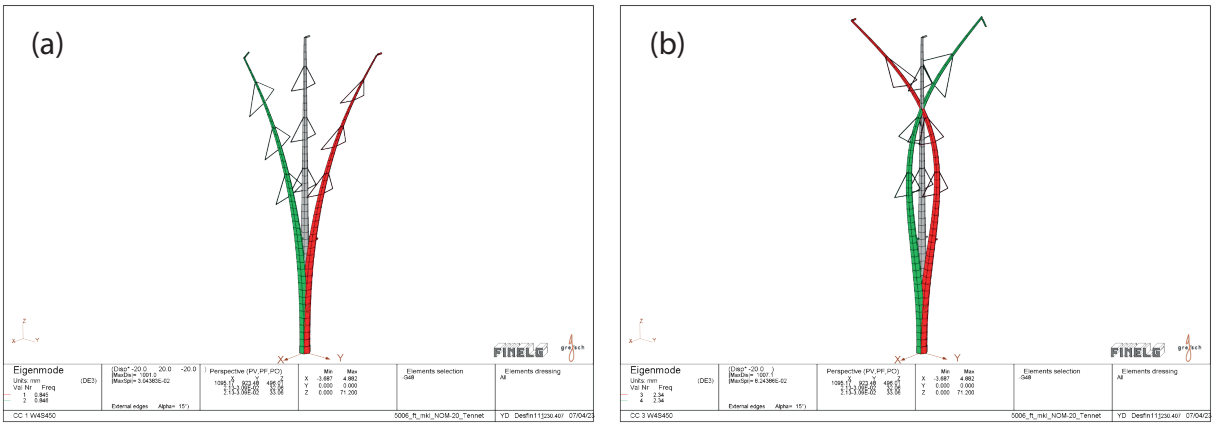


**Figure 2.** Mode shapes: (a) mode 1 (red), mode 2 (green); (b) mode 3 (green), mode 4 (red).

*3.2. Wind turbulence data*

Regarding wind turbulence data, since on-site measurements were not available, EC recommended values were considered. Interested readers can refer to [9] for detailed information. Table 3.2 shows detailed values of some quantities of importance in such an approach.

| $v_{ref}$ [m/s] | $c_{prob}$ [-] | $k_r$ [-] | $\alpha$ |
|---|---|---|---|
| 27 | 1.12 | 0.21 | 0.59 |

**Table 2.** Wind turbulence data used for Eurocode approach.

A terrain roughness of category II with $z_0 = 0.2$m and $z_{min} = 4$m were adopted. A return period of 500 years was assumed as of the client's request.

| | $u(t)$ | $v(t)$ | $w(t)$ |
|---|---|---|---|
| $\sigma$ [m/s] | 6.34 | 4.76 | 3.17 |
| $L_x$ [m] | 120 | 30 | 10 |
| $L_y$ [m] | 40 | 30 | 7.5 |
| $L_z$ [m] | 30 | 7.5 | 7.5 |

**Table 3.** Standard deviation and wind scale values for spatial wind turbulent components.

A common coherence coefficient $C = 10$ has been considered for all turbulence components, in all spatial directions.

*3.3. Description of the previous analyses*

Originally, the study was carried for comparing two types of wind analyses:

- Equivalent Static wind Loads approach from EN 1991-1-4 ([9]). It corresponds to the results under mean wind speed multiplied by a factor $(1 + 7I_u)C_sC_d \geq 1$ which accounts for the wind turbulent component. These values are computed at the pylon reference

height $z_{ref} = 0.6 z_{max} = 0.6 \cdot 71.2$m. With a turbulence intensity of $I_u = 0.186$ (i.e. 18.6%), $C_s C_d = 0.9$, the Eurocode extreme values correspond to the mean wind speed values multiplied by 2.07.

- A turbulent wind analysis by means of a spectral method, as of Eqs. (3) and (5).

Figure 3 shows the drag force coefficients, mean wind speeds, and the resulting equivalent wind forces along the tower's elevation.

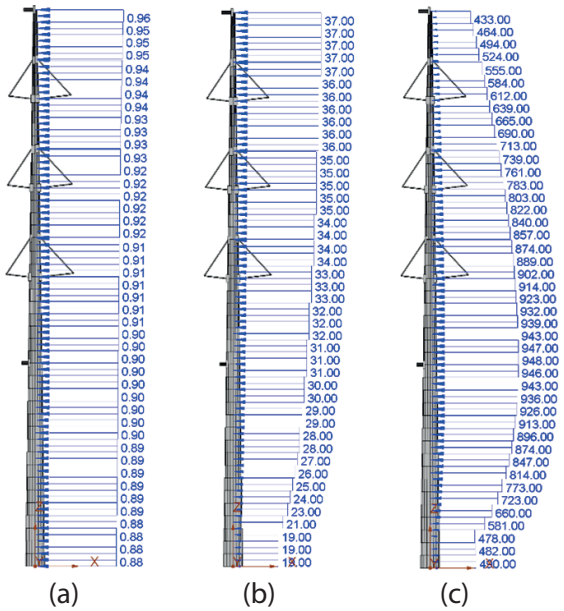


**Figure 3.** Eurocode equivalent static load approach. Variation along the tower height of: (a) $C_f$ wind force drag coefficient; (b) $V_m$ [m/s] mean wind speed; (c) $F_b$ [N/m] mean wind force (per unit length).

## 4. Results

In this application, three different approaches were adopted:

(i) Eurocode equivalent static loads;

(ii) Spectral analysis;

(iii) Bispectral analysis, as an extension of the spectral approach for non-Gaussian winds.

As stated in previous sections, the first two were already object of study and comparison of the design office. The third one is the new one proposed in this paper.

In the following illustrations, some label will be used in order to uniquely identify results from each one of the approaches explored in this application. For clarity, they are:

**EC** : Eurocode approach, equivalent static load method;

**ST** : stationary (mean) contribution of the wind action, obtained through a static analysis;

**TU** : turbulent (fluctuating) contribution, in both Gaussian and non-Gaussian context ($\text{TU}_{ng}$).

Indeed, combining ST with TU results in the extreme values of the response due to, Gaussian or non-Gaussian, wind action:

$$x_{max} = \overline{x} + g\ \sigma_x \tag{10}$$

where $\overline{x}$ is the average response value (ST label), $g$ the Gaussian (or non-Gaussian) peak factor, $\sigma_x$ its standard deviation [7] (i.e. label TU refers, in general, to $g\sigma_x$).

Figures 4 and 5 show the PSD and bispectrum of the nodal displacements of (i) a point at around the mid height of the pylon, and (ii) its top. Indeed, the amplitude (in absolute values) of both the spectrum and bispectrum are greater for the top node. This is the consequence of the fact that the structure behaves as cantilever-beam-like, for which the first vibration mode (in the along-wind direction) happens to be the most significant one. Nevertheless, second mode of vibration also show some small contribution to the overall structural response. This effect is much clearer for power spectrum, while at third order, this contribution almost flattens out.

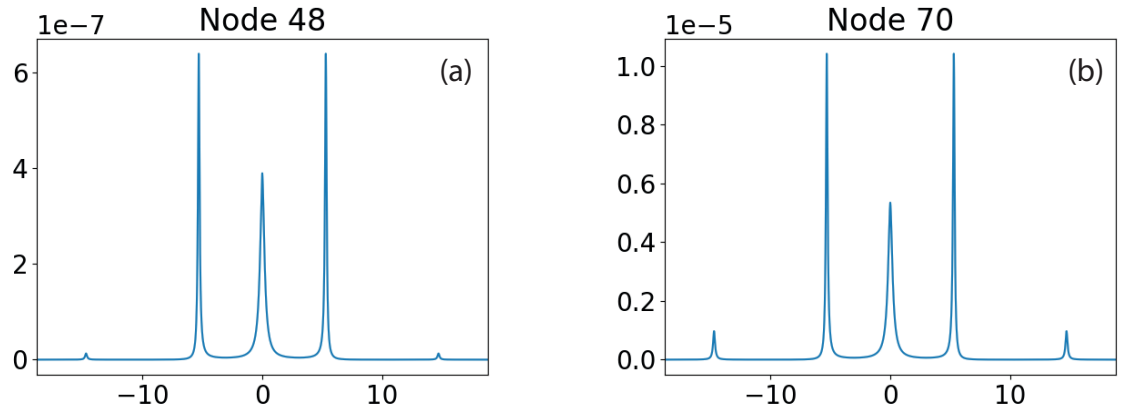


**Figure 4.** PSDs of the displacement along X: (a) point around the mid pylon height; (b) top point.

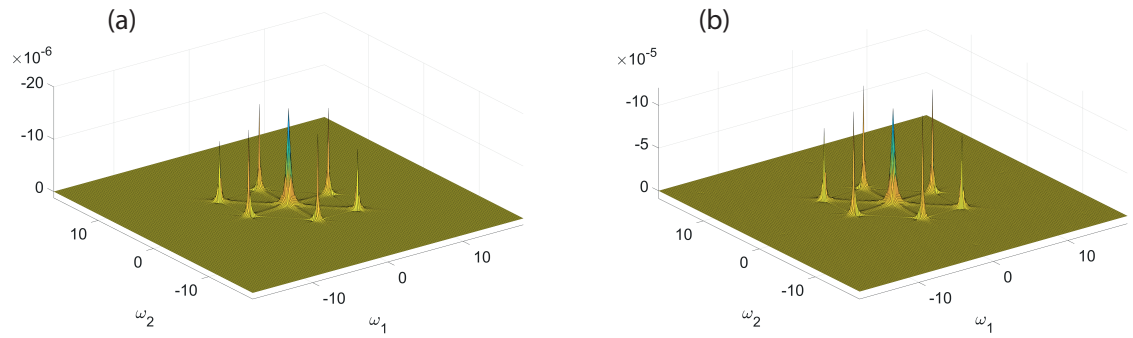


**Figure 5.** Bispectrum of the displacement along X: (a) point around the mid pylon height; (b) top point.

Figures 6 and 7 show the extreme values of bending moments and shear forces, along the pylon's height.

Table 4 finally compares the bending moment values at the bottom of the mast, computed with the the different approaches.

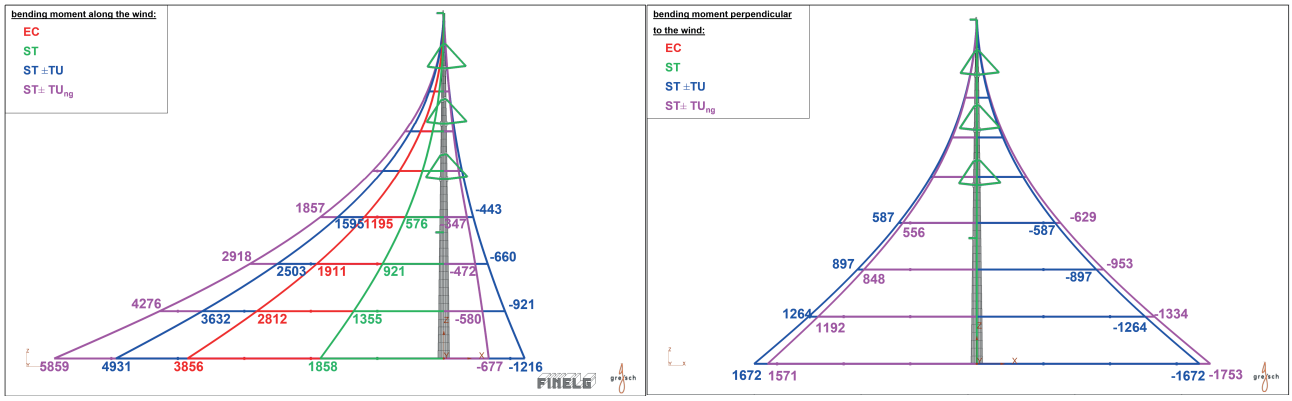


**Figure 6.** Extreme values of bending moments: along-wind (left); across-wind (right). EC = Eurocode approach; ST = Stationary (mean) part; TU = Turbulent part (Gaussian peak factor); $TU_{ng}$ = Turbulent part (non-Gaussian peak factors).

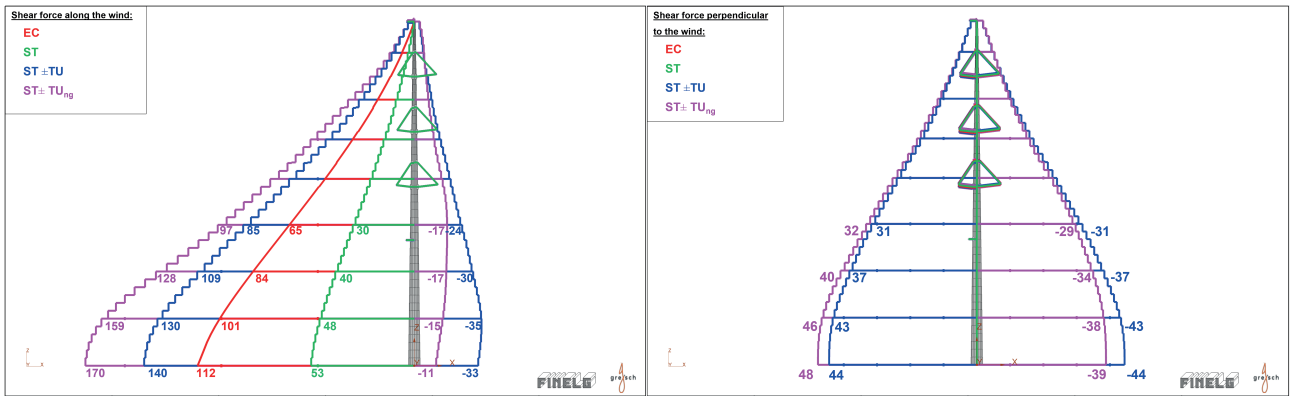


**Figure 7.** Extreme values of shear forces: along-wind (left); across-wind (right). EC = Eurocode approach; ST = Stationary (mean) part; TU = Turbulent part (Gaussian peak factor); $TU_{ng}$ = Turbulent part (non-Gaussian peak factors).

| | Bending moment along-wind [kNm] | Bending moment across-wind [kNm] | Shear force along-wind [kN] | Shear force across-wind [kN] |
|---|---|---|---|---|
| EC | 3855.6 | 0 | 112.29 | 0 |
| ST | 1857.7 | 0 | 53.44 | 0 |
| ST - TU | -1216.0 | -1672.3 | -33.11 | -44.391 |
| ST + TU | 4931.4 | 1672.3 | 139.99 | 44.391 |
| ST - $TU_{ng}$ | -676.5 | -1753.1 | -11.34 | -38.814 |
| ST + $TU_{ng}$ | 5858.8 | 1571.4 | 170.41 | 47.751 |

**Table 4.** Resume of numeric results for bending moment and shear force extreme values.

## 5. Conclusions

In the specific case of high-voltage pylons, when comparing results, it is found that turbulent wind analysis using the Gaussian model results in approximately 30% higher responses compared to the Eurocode equivalent static load method. Clearly, this discrepancy does not result from the main assumption made in the Eurocode equivalent approach of first mode modal truncation,

since as also shown from the spectra (PSD and bispectrum) from the more complete and accurate stochastic analyses, response contribution come mainly from first vibration mode, with residual from the second one. Furthermore, considering the actual non-Gaussian nature of wind effects increases the responses by an additional 20%. The extreme values obtained from a bispectral analysis are therefore approximately 50% than those estimated via the Eurocode approach. Therefore, in this application, results show how neglecting the non-Gaussian nature of wind loads, maximum (resp. minimum) responses are underestimated (resp. overestimated) in the Gaussian assumption, yielding to unsafe (resp. uneconomic) structural design.

**Acknowledgements**
Part of this research project has been supported thanks to a research project funded by the Walloon Region (Convention Nb. 8096, FINELG2020).

**References**

[1] S. Benfratello, G. Falsone, and G. Muscolino. "Influence of the quadratic term in the alongwind stochastic response of SDOF structures." In: *Engineering Structures* 18 (1996), pp. 685–695.

[2] Vincent Denoël. "On the background and biresonant components of the random response of single degree-of-freedom systems under non-Gaussian random loading". In: *Engineering Structures* 33.8 (2011), pp. 2271–2283.

[3] Vincent Denoël, Michele Esposito Marzino, and Margaux Geuzaine. "A multiple timescale approach of bispectral correlation". In: *Journal of Wind Engineering and Industrial Aerodynamics* 232 (2023).

[4] Michele Esposito Marzino and Vincent Denoël. "Non-Gaussian buffeting analysis of large structures by means of a Proper Orthogonal Decomposition". 2023.

[5] Massimiliano Gioffrè, Vittorio Gusella, and Grigoriu Mircea. "Non-Gaussian Wind Pressure on Prismatic Buildings." In: *Structural Engineering* 127 (2001), pp. 981–989.

[6] Ahsan Kareem and Teng Wu. "Wind-induced effects on bluff bodies in turbulent flows: Nonstationary, non-Gaussian and nonlinear features". In: *Journal of Wind Engineering and Industrial Aerodynamics* 122 (2013), pp. 21–37.

[7] Dae-Kun Kwon and Ahsan Kareem. "Peak Factor for Non-Gaussian Processes Revisited". In: *The Seventh Asia-Pacific Conference on Wind Engineering*. Nov. 2009.

[8] Loren D Lutes and Shahram Sarkani. "Random vibrations: analysis of structural and mechanical systems". In: Butterworth-Heinemann, 2004.

[9] *EN 1991-1-4:2005+A1 Eurocode 1: Actions on structures - Part 1-4: General actions - Wind actions*. EN. Brussels: CEN, 2009.